Protein Interaction Profiling of the p97 Adaptor UBXD1 Points to a Role for the Complex in Modulating ERGIC-53 Trafficking*[S]

Dale S. Haines‡§, J. Eugene Lee¶, Stephen L. Beauparlant‡, Dane B. Kyle‡, Willem den Besten¶, Michael J. Sweredoski‖, Robert L. J. Graham‖, Sonja Hess‖, and Raymond J. Deshaies¶**

UBXD1 is a member of the poorly understood subfamily of p97 adaptors that do not harbor a ubiquitin association domain or bind ubiquitin-modified proteins. Of clinical importance, p97 mutants found in familial neurodegenerative conditions Inclusion Body Myopathy Paget's disease of the bone and/or Frontotemporal Dementia and *A*myotrophic *L*ateral *S*clerosis are defective at interacting with UBXD1, indicating that functions regulated by a p97-UBXD1 complex are altered in these diseases. We have performed liquid chromatography-mass spectrometric analysis of UBXD1-interacting proteins to identify pathways in which UBXD1 functions. UBXD1 displays prominent association with ERGIC-53, a hexameric type I integral membrane protein that functions in protein trafficking. The UBXD1-ERGIC-53 interaction requires the N-terminal 10 residues of UBXD1 and the C-terminal cytoplasmic 12 amino acid tail of ERGIC-53. Use of p97 and E1 enzyme inhibitors indicate that complex formation between UBXD1 and ERGIC-53 requires the ATPase activity of p97, but not ubiquitin modification. We also performed SILAC-based quantitative proteomic profiling to identify ERGIC-53 interacting proteins. This analysis identified known (*e.g.* COPI subunits) and novel (Rab3GAP1/2 complex involved in the fusion of vesicles at the cell membrane) interactions that are also mediated through the C terminus of the protein. Immunoprecipitation and Western blotting analysis confirmed the proteomic interaction data and it also revealed that an UBXD1-Rab3GAP association requires the ERGIC-53 binding domain of UBXD1. Localization studies indicate that UBXD1 modules the subcellular trafficking of ERGIC-53, including promoting movement to the cell membrane. We propose that p97-UBXD1 modulates the trafficking of ERGIC-53-containing vesicles by controlling the interaction of transport factors with the cytoplasmic tail of ERGIC-53. ***Molecular & Cellular Proteomics 11: 10.1074/mcp.M111.016444, 1–11, 2012.***

P97 (also called VCP for valosin-containing protein or Cdc48 in yeast) is a highly conserved and abundant protein and is a member of the AAA (ATPases Associated with diverse cellular Activities) family of ATPases. The ATPase is mutated in two familial diseases, Inclusion Body Myopathy Paget's disease of the bone and/or Frontotemporal Dementia (IBMPFD)[1] and Amyotrophic Lateral Sclerosis (ALS), both of which display accumulation of ubiquitin positive vacuoles in affected cell types (1, 2). The protein functions in numerous cellular pathways, including homotypic membrane fusion, ERAD (ER-Associated Degradation), mitotic spindle disassembly, degradation of protein aggregates by autophagy and endo-lysosomal sorting of ubiquitinated caveolins (reviewed in 3–7, 8, 9, 10). Interestingly, the later two pathways are altered in cells transfected with mutant *P97* alleles derived from patients as well as in cells isolated from individuals harboring *P97* mutations (8, 9, 10).

P97 exists as a hexamer, with two centrally localized ATPase domains (reviewed in 3–7). It is thought that p97 uses energy derived from ATP hydrolysis to apply mechanical force on substrates, thereby changing their conformation and allowing for subsequent biochemical events. To date, p97 has been shown to function primarily on ubiquitinated proteins. Depending on the substrate, p97 can promote substrate deubiquitination (11), additional ubiquitination (12), proteasome delivery (13), and protein complex disassembly (14). Although p97 has been shown to act on ubiquitinated substrates, it does not directly bind ubiquitin or ubiquitin chains with high affinity (15). This activity is mediated by adaptors that harbor an ubiquitin association domain (UBA) and a p97-docking module. Numerous adaptors have been identified, including those having PUB, SHP, UBD, UBX, VBM, and VIM p97

From the ‡Fels Institute for Cancer Research and Molecular Biology and §Department of Biochemistry, Temple University School of Medicine, 3307 North Broad Street, Philadelphia, 19104 Pennsylvania; ¶Howard Hughes Medical Institute and ‖Proteome Exploration Laboratory; Beckman Institute, California Institute of Technology, 1200 E California Blvd. Pasadena, 91125 California

Received December 12, 2011
Published, MCP Papers in Press, February 14, 2012, DOI 10.1074/mcp.M111.016444

[1] The abbreviations used are: IBMPFD, Inclusion Body Myopathy Paget's disease of the bone and/or Frontotemporal Dementia; ALS, Amyotrophic Lateral Sclerosis; UBA, ubiquitin associated.

interaction motifs (reviewed in 16, 17, 18). The majority of these adaptors interact with the N-terminal domain of p97. Interestingly, over half of the mammalian UBX-domain containing proteins (the largest family of adaptors) do not harbor an UBA domain, nor bind ubiquitinated proteins (19). There is currently very little information pertaining to the activities of proteins that comprise this sub-family of p97 adaptors.

The biochemical mechanism by which disease-relevant *P97* mutations alter the function of the ATPase is not well understood. Some of the mutations that cause IBMPFD stimulate the ATPase activity of p97 (20). Other studies indicate that they alter the binding of specific adaptors to the N-terminal domain of p97, where most of the IBMPFD mutations are found (21). Intriguingly, these alterations can both promote the binding of certain adaptors and suppress the interaction with others (21). UBXD1, a member of the non-UBA family of p97 adaptors, has recently been shown to be deficient at interacting with several p97 mutants, including those commonly found in familial IBMPFD and ALS (10). This study also demonstrated that UBXD1 collaborates with p97 in the endo-lysosomal sorting of ubiquitinated caveolins and this process is altered in cells containing mutant p97 (10). To gain further insights into the pathways in which p97-UBXD1 complex functions, we used immunopurification and mass spectrometric methods to identify proteins that associate with UBXD1. The results obtained with these methods as well as follow-up protein interaction and localization studies indicate that p97-UBXD1 modulates the subcellular localization of ERGIC-53 containing vesicles.

MATERIALS AND METHODS

Plasmids and Antibodies—Supplementary Table S1 describes plasmids used in this study and how they were generated. Constructs encoding amino-terminal FLAG tagged adaptors have been described previously (19). Antibodies used in experiments presented here are anti-FLAG mouse monoclonal antibody M2 (SIGMA), anti-UBXD1 mouse monoclonal antibody 5C3–1 (22), anti-ERGIC-53 H-245 rabbit polyclonal (Santa Cruz, Santa Cruz, CA), anti-p97 H-120 rabbit polyclonal (Santa Cruz), anti-Rab3GAP1 rabbit polyclonal (Novus, Littleton, CO), and anti-Rab3-GAP2 rabbit polyclonal (GeneTex, San Antonio, TX).

Ponasterone-inducible System and Transient Transfections—The human lung adenocarcinoma cell line H1299 was first transfected by the calcium phosphate method with the pVgRXR plasmid (Invitrogen, Carlsbad, CA). Cells were cultured in 400 μg/ml zeocin until visible colonies were evident. Fourteen colonies were isolated, expanded, and tested for ponasterone inducibility using a transiently transfected pIND-LacZ reporter (Invitrogen) and liquid β-galactosidase assay. The clone (#9) giving the best inducibility and the lowest background in the absence of ponasterone was transfected by calcium phosphate with a second pVgRXR construct that harbors an introduced puromycin resistance gene. Cells were cultured in the presence of zeomycin (400 μg/ml) and puromycin (0.5 μg/ml) until visible colonies were present. Twenty-two colonies were isolated, expanded, and tested for ponasterone inducibility as described above. The clone (#9–8) giving the best inducibility with the lowest background was transfected by FuGENE6 (Roche) with pIND (Invitrogen) and pIND-UBXD1^{FLAG} expression constructs. Cells were cultured in the presence of zeomycin (400 μg/ml), puromycin (0.5 μg/ml), and hygromycin (200 μg/ml) for 2 weeks to generate a pool of stably transfected cells. To induce UBXD1^{FLAG} expression, cells were exposed to the noted concentration of ponasterone for 24–48 h. For experiments using transiently transfected cells, H1299 or Hek 293Ts (293T) were transfected with the indicated amount of DNA using FuGENE6 (Roche) according to the manufacturer's instructions. Cells were harvested or treated with inhibitors 48 h after exposure to plasmid DNA-FuGENE6 mixtures.

Mass Spectrometric Analyses—Mass spectrometry was performed as described previously (23). Briefly, cell pellets were collected and lysed in lysis buffer (50 mM HEPES, pH 7.5; 70 mM KOAc; 5 mM $Mg(OAc)_2$; 0.2% n-dodecyl-β-D-maltoside) containing 1 $\times$ protease inhibitor tablet (Roche) for 30 min on a nutator at 4 °C. The lysates were centrifuged at 16,600 $\times$ *g* for 15 min to remove cell debris, and the supernatant was incubated with anti-FLAG beads on a nutator for 1 h at 4 °C. Beads were washed with lysis buffer 5 times, followed by 2 washes with 100 mM Tris-HCl (pH 8.5). Proteins were eluted from beads in 10 M freshly prepared urea. Digestion was performed in 100 mM Tris-HCl (pH 8.5) containing 8 M urea at 37 °C first with Lys-C (35 ng/mg lysate) for 4 h, and then the urea concentration was reduced to 2 M for trypsin (30 ng/mg lysate) digestion overnight. Following digestion, the tryptic peptides were desalted on a reversed-phase Vivapure C18 micro spin column (Sartorius Stedim Biotech, Gottingen, Germany) and concentrated using a SpeedVac. Dried samples were acidified by 0.2% formic acid prior to liquid chromatography-mass spectrometric analysis.

All liquid chromatography-mass spectrometry experiments were performed on an EASY-nLC (Thermo Scientific, West Palm Beach, FL) connected to a hybrid LTQ Orbitrap Classic or LTQ FT (Thermo Scientific) equipped with a nano-electrospray ion source (Thermo Scientific). Peptides were separated on a 15-cm reversed phase analytical column (75 μm internal diameter) in-house packed with 3 μm C18AQ beads (ReproSil-Pur C_{18AQ}) using a 120-min gradient from 13% to 25% acetonitrile in 0.2% formic acid at a flow rate of 350 nL/minute. The mass spectrometer was operated in data-dependent mode to automatically switch between full-scan MS and tandem MS acquisition. Survey full scan mass spectra were acquired in Orbitrap or FT (300–1700 *m/z*), after accumulation of 500,000 ions, with a resolution of 60,000 at 400 *m/z*. The top ten most intense ions from the survey scan were isolated and, after the accumulation of 5000 ions, fragmented in the linear ion trap by collisionally induced dissociation (collisional energy 35% and isolation width 2 Da). Precursor ion charge state screening was enabled and all singly charged and unassigned charge states were rejected. The dynamic exclusion list was set with a maximum retention time of 90 s, a relative mass window of 10 ppm and early expiration was enabled.

For data analysis, peaks were generated from raw data files using MaxQuant (version 1.2.2.5) with default parameters (24) and searched using the built-in search engine Andromeda (25). Peak lists were searched against the International Protein Index (IPI) human database (version 3.54, 75448 sequences) and a contaminant database (262 sequences). The search parameters were tryptic digestion, maximum of two missed cleavages, fixed carboxyamidomethyl modifications of cysteine, variable oxidation modifications of methionine, and variable protein N-terminal carbamylations. SILAC samples were searched with Arg6 and Lys8 as variable modifications as well. Mass tolerance for precursor ions were 7 ppm and that for fragment ions were 0.5 Da. Protein inference and quantitation were performed by MaxQuant with 1% false discovery rate thresholds for both peptides and proteins as calculated using a decoy search. Additionally, at least two different peptide sequences were required for protein identification. No threshold was employed for individual MS/MS spectra because we were

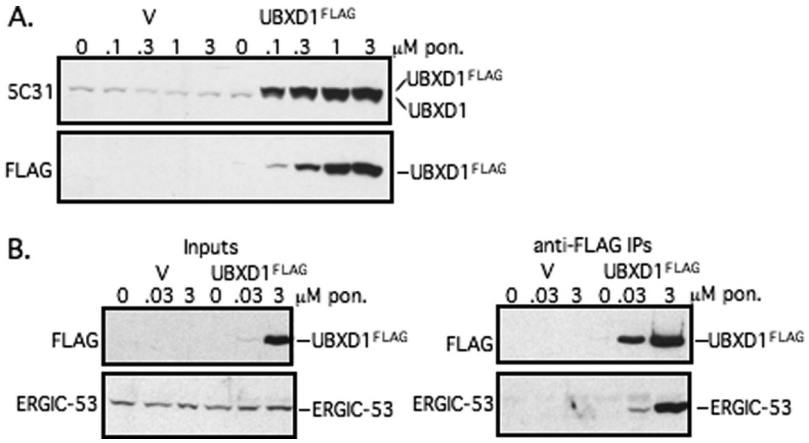

FIG. 1. **ERGIC-53 is a UBXD1 interacting protein.** *A*, H1299 cells harboring pIND (V) and pIND-UBXD1^{FLAG} were generated and exposed to varying doses of ponasterone. Extracts were prepared and Western blots carried out with anti-UBXD1 (5C31) and anti-FLAG antibodies. *B*, Extracts prepared from mock and induced cells were subjected to anti-UBXD1 immunoprecipitation, followed by western bots with anti-FLAG and anti-ERGIC-53 antibodies.

primarily interested in protein identification and not specific peptide sequences or post-translational modifications. Peptides were assigned to proteins using the principle of maximum parsimony. Additionally, protein groups were formed where there was no evidence to disambiguate protein isoforms. Relative protein amounts were semi-quantitatively measured using spectral counts using all peptides (distinct and shared) within a protein group. In the case of SILAC experiments, spectral counting was still employed because H/L ratios were often incalculable because of the binary nature of the experiments. To identify proteins with spectral counts significantly different, binomial tests were performed assuming equal probability of observation in either case (*i.e.* bait or empty, heavy or light). Proteins were determined to be significant if their p value was lower than the Bonferroni adjusted threshold of $0.05/n$ where n is the number of tests performed. Complete files of the proteomic analysis are presented in supplementary Tables S1 to S5.

Immunoprecipitations and Western Blotting—Cell pellets were lysed in EBC (50 mM Tris-HCl pH7.5, 120 mM NaCl, 1% Nonidet P-40) or n-dodecyl-β-D-maltoside-based buffer (see previous section) supplemented with protease inhibitors for 15 min at 4 °C. Extracts were subjected to centrifugation and supernatants transferred to a new tube. Protein concentration was determined by the Bradford method using a kit from Bio-Rad. For immunoprecipitations, samples containing 0.5–1 mg of lysate were incubated with anti-FLAG beads for 1–3 h on a nutator at 4 °C. Beads were then pelleted, washed three times in lysis buffer, resuspended in 1 × SDS-PAGE loading buffer and placed at 95 °C for 5 min. Proteins were resolved by SDS-PAGE in running buffer (250 mM Glycine, 25 mM Tris, 0.1% SDS) and transferred to nitrocellulose membranes in methanol-containing transfer buffer (200 mM Glycine, 25 mM Tris, 20% Methanol) for 1 h at 125 V. Membranes were then washed in phosphate-buffered saline (PBS)-Tween-20 (PBS-T) (63 mM Na_2HPO_4, 15.5 mM NaH_2PO_4, 7.5 mM NaCl, 0.1% Tween-20) and blocked in 5% milk in PBS-T for 1 h at room temperature. Primary antibodies were added at appropriate dilutions in 5% milk in PBS-T and rocked overnight at 4 °C. Following primary antibody, membranes were washed and incubated with secondary antibody (at appropriate dilution) in 5% milk in PBS-T for an hour. Membranes were washed and treated with Western Lightning Plus - ECL (PerkinElmer) as per manufacturer's instructions. Chemiluminescence was detected by exposure on X-ray film.

Immunofluorescence—Cells were grown to 40% confluency on glass cover slips that had been placed in six-well plates. Cells were washed twice in PBS, and then fixed in 4% paraformaldehyde PBS for 15 min. Samples were washed twice in PBS. Samples were blocked for 1 h at room temperature in blocking solution (10% FBS, 0.1% Triton X-100 in PBS). After two more washes in PBS, samples were incubated in primary antibodies (0.5 ml of 10% fetal bovine serum in PBS) for 1 h at 37°C with gentle rocking. After two more PBS washes, samples were incubated in secondary antibodies (0.5 ml of 10% FBS in PBS) for 45 min at 37°C. After the final 2 washes in PBS, cover slips were inverted onto glass slides with 1 drop mounting solution (SloFade Gold with DAPI, Invitrogen). Cells were visualized using a Leica TCS SP5 confocal microscope. For confocal microscopy, all scans were created using sequential capture to prevent bleed through or cascading fluorescence. Excitation lasers and detection ranges are as follows: DAPI: 405 nm, 415 nm–476 nm; AlexaFluor 568 (ERGIC-53): 561 nm, 571 nm–638 nm; AlexaFluor 647 (UBXD1): 633 nm, 644 nm–703 nm. Images were modified and analyzed with either Spot Advanced sofware or LAS AF software. Post-processing of images obtained with LAS AF software consisted of mean baseline correction and medium noise reduction.

RESULTS

Mass spectrometric analysis identifies ERGIC-53 as a high abundance UBXD1 interacting protein. We first generated a H1299 derived cell line that allows for regulated expression control of a C-terminally FLAG-tagged UBXD1 protein (UBXD1^{FLAG}) using the *Drosophila* hormone ponasterone (Fig. 1*A*). After generation of this line, cells were exposed to two different concentrations (0.1 and 0.3 μM) of hormone, which results in modest overexpression of UBXD1^{FLAG} (in the two-fivefold range over endogenous UBXD1) (Fig. 1*A*). UBXD1^{FLAG} and interacting proteins were immunopurified from extracts using anti-FLAG antibody-conjugated beads and subjected to mass spectrometric analysis using an LTQ-FT instrument. Table I provides a list of proteins present in the UBXD1^{FLAG} samples and not present in control anti-FLAG immunoprecipitations from mock-induced cells harboring the empty vector. As expected, UBXD1 and p97 were abundant constituents of both UBXD1^{FLAG} immunoprecipitates. The protein that yielded the next highest number of spectra counts was ERGIC-53. Also present in both UBXD1^{FLAG} immunoprecipitations was the actin binding protein LIMA1 (also called EPLIN1), SEPT9 and DST (Table I). CAV1, a recently identified UBXD1 interacting protein (10), was detected but the number of spectral counts for CAV1 was low and did not reach statistical significance.

TABLE I

*Spectral counts of proteins associated with UBXD1^{FLAG} upon ponasterone induction in H1299 cells.[a] *Indicates significant enrichment in UBXD1^{FLAG} immunoprecipitations ($p < 0.05$ Bonferroni corrected)*

Proteins[b]	# of assigned spectra[c]	
	0.1 μM	0.3 μM
Transitional endoplasmic reticulum ATPase (VCP; p97)	183*	512*
UBX domain-containing protein 1 (UBXD1)	74*	89*
ER-Golgi intermediate compartment 53kDa protein (ERGIC-53)	33*	34*
Epithelial protein lost in neoplasm (EPLIN, LIMA1)	6	22*
SEPT9 protein (SEPT9)	3	16*
Dystonin (DST)	8	13*

[a] Mass spectrometry was performed with LTQ-FT instrument.
[b] Peptides and proteins were filtered at a 1% false discovery rate.
[c] Inclusion limit set at a minimal of 10 spectra counts for 0.3 μm.

In addition to performing the analysis with the inducible H1299 system, we characterized ^{FLAG}UBXD1 interacting proteins using transiently transfected 293T cells. For these studies, we used SILAC (stable isotope labeling with amino acids in culture) and an LTQ-Orbitrap instrument. Samples were comprised of a 1:1 mixture of FLAG immunoprecipitates from "light" 293T cells (cultured in media supplemented with standard lysine and arginine) that had been transiently transfected with UBXD1^{FLAG} plasmid *versus* "heavy" 293T cells (cultured in media containing Arg6 (U-^{13}C6) and Lys8 (U-^{13}C6, U-^{15}N2)) that had been transfected with the empty vector control. Table II provides a list of proteins that were present in UBXD1^{FLAG} immunoprecipitates. These proteins were not found in the control immunoprecipitations (*i.e.* no heavy peptides found). P97, UBXD1 and ERGIC-53 were present at high abundance. Numerous proteins were also identified in this second round of analysis, including 3 additional p97 interacting proteins (UBXD8, UBXD9, NPL4), ERGIC-53 binding proteins (MCFD2 and COPA) and others with diverse functions (CAD, ATP5B, PRKDC, IRS4, FLOT1). We also found high abundance proteins that are routinely found in shotgun mass spectrometry experiments, including ribonucleotide protein HNRNPU, translation elongation factor EEF1A2, transcription factors RUVBL1 and RUVBL2 and components of various chaperone systems (GRP78, UGGT1, HSPA1A, CCT8). TUBA1C and TUBB6 were identified as well, which is interesting as numerous tubulin proteins were later found to be highly enriched in ^{FLAG}ERGIC-53 immunoprecipitations.

We decided to focus our follow-up studies on ERGIC-53, the most dominant novel UBXD1^{FLAG} interacting protein identified in the three different experiments. ERGIC-53 is a mannose-binding ER resident protein that participates in the early part of the secretory pathway (reviewed in 26, 27). It contains a single-pass transmembrane domain oriented such that the vast majority of the molecule is present in the lumen of the ER, with only 12 C-terminal residues at the C terminus exposed to the cytosol. Like p97, ERGIC-53 exists as a hexamer. The current working model is that ERGIC-53 binds ER-localized client proteins on its own or via its co-factor MCFD2. Upon client binding, ERGIC-53 undergoes COPII-dependent budding from the ER, which requires its C-terminal diphenylalanine motif. ERGIC-53 containing vesicles then move to a structure called the ER-Golgi Intermediate Compartment (ERGIC), where they fuse and deliver client proteins for further sorting and trafficking. ERGIC-53 is recycled from the ERGIC to the ER by COPI-complex-dependent budding, which is specified by two lysine residues that precede the C-terminal phenylalanine residues.

TABLE II

Spectral counts of proteins associated with UBXD1^{FLAG} in transiently transfected 293T cells as assessed by SILAC[a]

Proteins[b]	# of assigned spectra[c]
Transitional endoplasmic reticulum ATPase (VCP; p97)	598
UBX domain-containing protein 1 (UBXD1)	403
ER-Golgi intermediate compartment 53kDa protein (ERGIC-53)	103
Tubulin alpha-1C chain (TUBA1C)	75
Aspartate carbamoyltransferase (CAD)	55
RuvB-like 2 (RUVBL2)	52
78 kDa glucose-regulated protein (GRP78)	48
UBX domain-containing protein 9 (UBXD9)	37
UDP-glucose:glycoprotein glucosyltransferase 1 (UGGT1)	33
Heat shock 70 kDa protein 1A/1B (HSPA1A,HSPA1B)	33
cDNA FLJ54303, highly similar to Heat shock 70 kDa protein 1	30
UBX domain-containing protein 8 (UBXD8)	28
Elongation factor 1-alpha 2 (EEF1A2)	29
cDNA FLJ52712, highly similar to Tubulin beta-6 chain (TUBB6)	29
RuvB-like 1 (RUVBL1)	27
Tubulin beta-6 chain (TUBB6)	27
ATP synthase subunit beta, mitochondrial (ATP5B)	23
40S ribosomal protein S3 (RPS3)	20
DNA-dependent protein kinase catalytic subunit (PRKDC)	19
T-complex protein 1 subunit theta (CCT8)	19
Insulin receptor substrate 4 (IRS4)	18
Nuclear protein localization protein 4 homolog (NPL4)	17
Calnexin (CANX)	17
Flotillin-1 (FLOT1)	15
Heterogeneous nuclear ribonucleoprotein U (HNRNPU)	15
Multiple coagulation factor deficiency protein 2 (MCFD2)	14
Coatomer subunit alpha (COPA)	13

[a] Mass spectrometry was performed with LTQ-orbitrap instrument.
[b] Peptides and proteins were filtered at a 1% false discovery rate.
[c] Inclusion limit set at a minimal of 10 spectra counts and all proteins are significantly enriched in UBXD1^{FLAG} immunoprecipitations ($p < 0.05$ Bonferroni corrected).

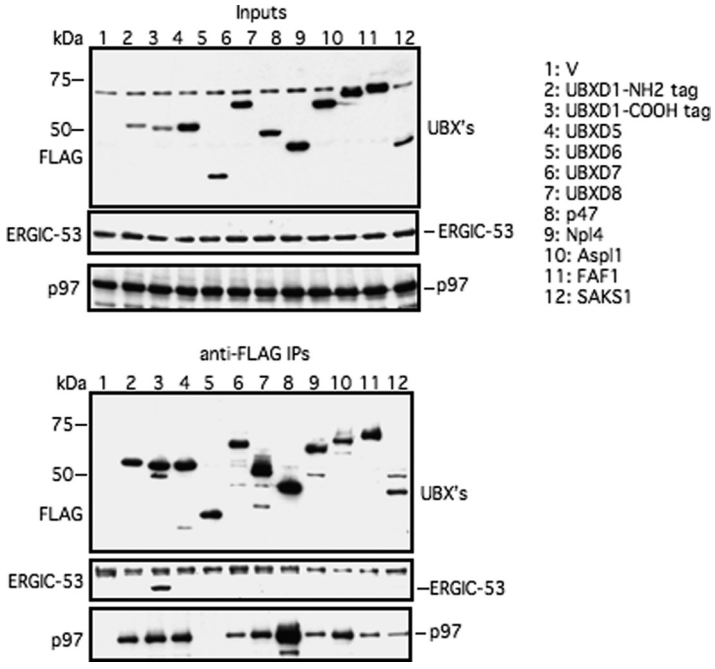

FIG. 2. **Specificity of UBXD1-ERGIC-53 interaction.** H1299's were transfected with 3 μg of the indicated FLAG-tagged expressions constructs. Extracts were prepared and immunoprecipitations carried out with anti-FLAG beads. Western blots were then performed with anti-FLAG, anti-ERGIC-53, and anti-p97 antibodies.

We first sought to validate the mass spectrometry findings by conventional immunoprecipitation and Western blotting. Two concentrations of ponasterone were used for this verification experiment: one (0.03 μM) that results in the production of UBXD1^{FLAG} at physiologically relevant levels and another (3 μM) that results in ~10-fold overproduction (Fig. 1*A*). After induction, cells were harvested, extracts prepared, and immunoprecipitations carried out with anti-FLAG beads. Immunoprecipitated proteins were resolved by SDS-PAGE, transferred to nitrocellulose membranes and probed with anti-FLAG and anti-ERGIC-53 antibodies. As shown in Fig. 1*B*, endogenous ERGIC-53 was present in both anti-FLAG immunoprecipitates.

ERGIC-53 interacts specifically with UBXD1. We next assessed if ERGIC-53 associates with other UBX domain-containing p97 adaptors. For this experiment, expression constructs encoding 10 different FLAG-tagged UBX proteins were transiently transfected into H1299 cells. Protein extracts were prepared and immunoprecipitations using anti-FLAG beads were performed as described above. Western blotting was then carried out with FLAG, ERGIC-53, and p97 antibodies. As shown in Fig. 2, UBXD1^{FLAG} was the only UBX domain-containing adaptor that bound ERGIC-53.

N-terminal region of UBXD1 and C-terminal tail of ERGIC-53 are required for complex formation. During the course of testing for interactions between ERGIC-53 and the various p97 adaptors, we noticed that whereas UBXD1^{FLAG} was proficient at binding endogenous ERGIC-53, N-terminally-tagged ^{FLAG}UBXD1 was not (Fig. 2). These results raised the possibility that the N terminus of UBXD1 is important for ERGIC-53 binding. To test this idea, we generated a series of N-terminal UBXD1^{FLAG} deletion mutants and examined their ability to bind endogenous ERGIC-53 and p97 in transiently transfected H1299 cells. As shown in Fig. 3*A*, deletion of the first 10 amino acids of UBXD1^{FLAG} resulted in the loss of binding to ERGIC-53, but not p97. We next performed alanine-scanning mutagenesis to identify individual amino acids within this region that are required for ERGIC-53 association. Fig. 3*B* shows that mutating N-terminal residues 2, 4, 5, 7, and 8 compromised the ability of UBXD1^{FLAG} to associate with ERGIC-53.

Given the known topology of ERGIC-53 in the ER membrane, we reasoned that the last 12 amino acids of ERGIC-53 mediate binding to UBXD1. To test this, cells were co-transfected with constructs encoding C-terminally HA-tagged UBXD1 (UBXD1^{HA}) and expression plasmids encoding N-terminally FLAG-tagged ERGIC-53 (^{FLAG}ERGIC-53) or a mutant lacking the last 12 amino acids (^{FLAG}ERGIC-53ΔC). Extracts were prepared and immunoprecipitations were performed with anti-HA conjugated beads. Westerns were then carried out with anti-FLAG and anti-UBXD1 antibodies. As shown in Fig. 3*C*, deletion of the C-terminal 12 residues of ^{FLAG}ERGIC-53 resulted in the loss of UBXD1^{HA} binding.

UBXD1-ERGIC-53 association is suppressed by the p97 inhibitor DBeQ, but not the E1 ubiquitin activation enzyme inhibitor PYR-41. We next wanted to assess if the interaction between UBXD1 and ERGIC-53 requires the enzymatic function of the ATPase or ubiquitin modification. Cells harboring ponasterone-inducible UBXD1^{FLAG} were exposed to hormone for 6 h in the absence and presence of the p97 inhibitor DBeQ (28) or the E1 ubiquitin activation enzyme inhibitor PYR-41 (29). After treatments, cells were harvested, extracts were prepared, and immunoprecipitations performed with anti-

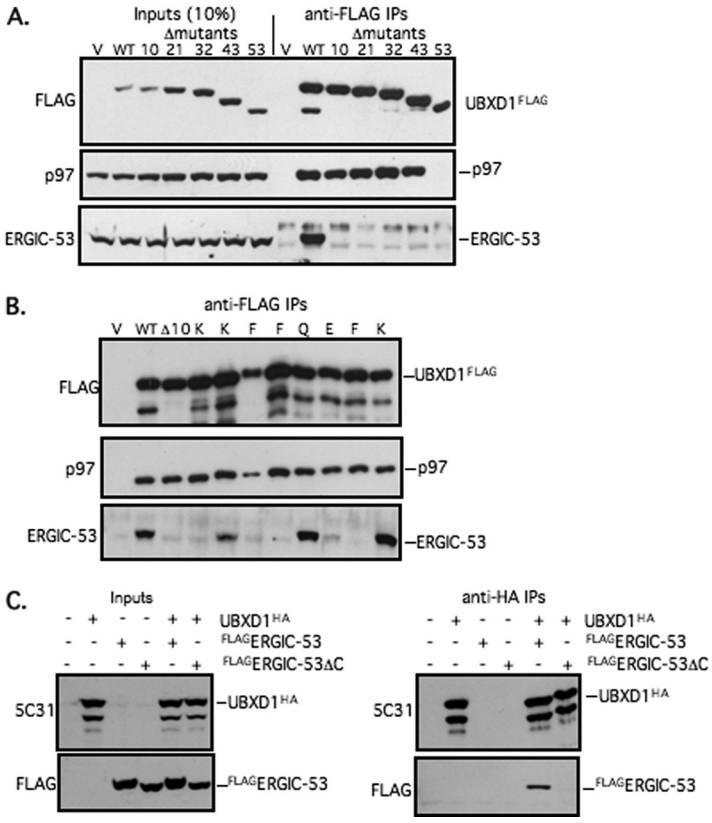

FIG. 3. **Defining domains/amino acids of UBXD1 and ERGIC-53 required for binding.** *A*, H1299 cells were transfected with 3 μg of expression constructs encoding UBXD1^{FLAG} or deletion mutants lacking the indicated number of amino-terminal amino acids. Extracts were prepared and immunoprecipitations carried out with anti-FLAG beads. Western blots were performed with anti-FLAG, anti-ERGIC-53, and anti-p97 antibodies. *B*, The experiment was performed as described in *A* with UBXD1^{FLAG} mutants harboring the indicated substitutions in the first 10 amino acids. *C*, 293T cells were transfected with 2 μg of UBXD1^{HA} expression construct and 2 μg of ^{FLAG}ERGIC-53 or ^{FLAG}ERGIC-53ΔC mutant lacking the last 12 amino acids of the protein. Extracts were prepared and immunoprecipitations carried out with anti-HA antibody conjugated beads. Western blots were performed with the indicated antibodies.

FLAG antibody. The amounts of endogenous ERGIC-53 in these immunoprecipitations was determined by Western blotting. As shown in Fig. 4*A*, treatment of cells with DBeQ suppressed an interaction between UBXD1^{FLAG} and ERGIC-53. The E1 ubiquitin activation enzyme inhibitor PYR-41 had no apparent effect on UBXD1^{FLAG} association with ERGIC-53. Similar results were obtained in 293T cells transiently transfected with UBXD1^{FLAG} (Fig. 4*B*). Treatment of transfected cells with 10 μM DBeQ for 8 h inhibited binding of endogenous ERGIC-53 to UBXD1^{FLAG}, without altering p97-UBXD1^{FLAG} interaction. PYR-41 exposure had no discernable effect on the binding of UBXD1^{FLAG} to ERGIC-53 (Fig. 4*B*).

Quantitative mass spectrometric analyses for ERGIC-53 interacting proteins. We next characterized the interactome for ERGIC-53. For these experiments, we performed SILAC mass spectrometric analysis of "light" labeled 293T cells that had been transfected with the ^{FLAG}ERGIC-53 expression construct *versus* "heavy" labeled 293T cells that had been transfected with the empty vector control. Table III provides a list of proteins that were detected in ^{FLAG}ERGIC-53 but not in control immunoprecipitates in two independent experiments. Interactions were detected with proteins that make up the COPI complex (COPA, COPB2, COP3, COPB1) as well as with Rab3GAP1 and Rab3GAP2. COPI proteins promote the retrograde transport of ERGIC-53 to the ER (30). Rab3GAP1 and Rab3GAP2 form a stable heteromeric complex and regulate the fusion of vesicles to the plasma membrane (31). Their interactions with ERGIC-53 have yet to be reported. Numerous tubulin proteins (TUBB2C, TUBB3, TUBB4, TUBB2, TUBB), which could play a role in facilitating transport of ERGIC-53 containing vesicles, were also present in ^{FLAG}ERGIC immunoprecipitations. Not surprisingly, a few chaperones were present in these immunoprecipitations as well, including HSPA8, HSPA1A/HSPA1B, and DNAJC7. Curiously, although we did identify p97 peptides in the ^{FLAG}ERGIC-53 immunoprecipitates, we did not detect UBXD1. There are a couple of possible explanations for this, including that the amount of interacting UBXD1 is below our detection limits and/or that p97 can interact with ERGIC-53 via UBXD1 independent mechanisms, perhaps even with misfolded polypetides during the process of ERAD. It is also curious that we did not identify any COPII proteins in this analysis. The percentage of ERGIC-

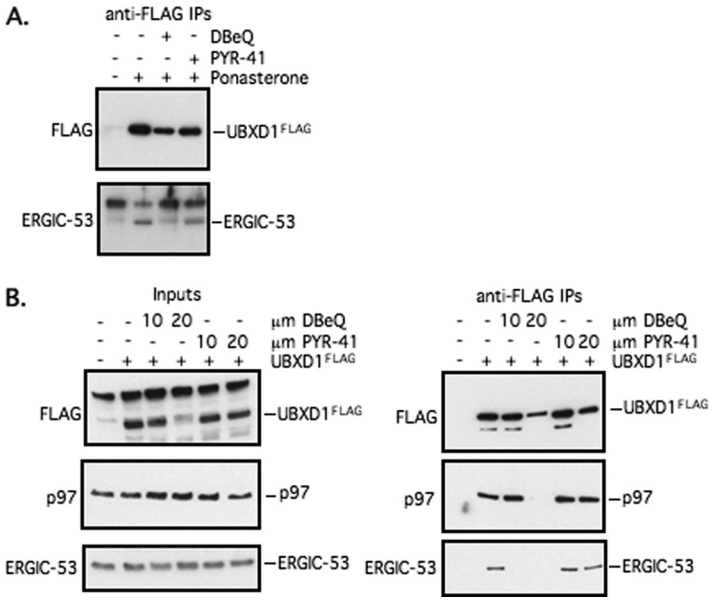

FIG. 4. **Effects of the p97 inhibitor DBeQ and the E1 ubiquitination activation enzyme inhibitor PYR-41 on UBXD1-ERGIC-53 interaction.** *A*, Cells harboring ponasterone-inducible UBXD1^{FLAG} were untreated or exposed to 3 μM ponasterone in the absence or presence of 10 μM DBeQ or 10 μM PYR-41 for 6 h. Cells were harvested, extracted prepared and immunoprecipitations performed with anti-FLAG beads. Western blots were then carried out with anti-FLAG and anti-ERGIC antibodies. *B*, 293T cells were transfected with 1 μg of FLAG-tagged UBXD1. Forty-eight hrs after transfections, cell were treated with the indicated concentration of DBeQ or PYR-1. Cells were harvested, extracted prepared and immunoprecipitations performed with anti-FLAG beads. Western blots were then carried out with anti-FLAG, anti-ERGIC-53, and anti-p97 antibodies.

53-COPII complexes at any one time may be small or just highly unstable under the conditions used here.

Identification of proteins that require the C-terminal tail of ERGIC-53 for binding. Considering that UBXD1 binds to the C-terminal tail of ERGIC-53 and may regulate interactions that also occur there, we next wanted to identify ^{FLAG}ERGIC-53 binding proteins that require this tail for association. SILAC-based quantitative proteomics was again performed, measuring the level of enriched ^{FLAG}ERGIC-53 interacting proteins in cells transfected with full length ^{FLAG}ERGIC-53 *versus* the C-terminal deletion mutant. Table IV displays a list of proteins whose peptide spectral counts were significantly decreased more than 3 fold in ^{FLAG}ERGIC-53ΔC immunoprecipitates as well as the ratio of known proteins that are part of these complexes that were in both ^{FLAG}ERGIC and ^{FLAG}ERGIC-53 immunoprecipitation. Rab3GAPs and COPI complex proteins were the only proteins found to require the C-terminal tail of ^{FLAG}ERGIC-53 for binding.

An interaction between ERGIC-53 and the Rab3GAP complex has yet to be reported and we thus wanted to verify this association by immunoprecipitation and Western blotting. We also wanted to test if UBXD1, ERGIC-53 and Rab3GAPs can form a ternary complex. As shown in Fig. 5, ^{FLAG}ERGIC-53 interacted with endogenous Rab3GAP1 and Rab3GAP2 and these associations were not observed with a ^{FLAG}ERGIC-53 mutant lacking the C-terminal 12 residues of the protein. Fig. 5 also shows that whereas RabGAP1 was present in UBXD1^{FLAG} immunoprecipitates, it was not present in those using the UBXD1Δ10^{FLAG} mutant that was unable to bind ERGIC-53. We were unable to detect Rab3GAP2 in the UBXD1^{FLAG} immunoprecipitations, presumably because of the insensitive nature of the anti-Rab3GAP2 antibody used here. Notwithstanding, these studies indicate that an ERGIC-53 hexamer can accommodate the docking of multiple protein complexes to its C-terminal tail.

UBXD1 modulates ERGIC-53 localization. As the C-terminal tail of ERGIC-53 plays an important role in controlling its localization in cells via interaction with various protein trafficking complexes (reviewed in 26, 27), we wanted to evaluate if UBXD1^{FLAG} expression influences the subcellular localization of ERGIC-53. We again used the ponasterone inducible system for this analysis and included cells that inducibly express the UBXD1Δ10^{FLAG} mutant that is ERGIC-53 binding deficient. Cells harboring the empty vector control, UBXD1^{FLAG} or UBXD1Δ10^{FLAG} were exposed to 1 μM ponasterone for 48 h. Cells were fixed and localization of endogenous ERGIC-53 and induced UBXD1^{FLAG} was determined by indirect immunofluorescence with rabbit anti-ERGIC-53 and mouse anti-UBXD1 antibodies. We observed two distinct types of altered ERGIC-53 localization phenotypes upon expression of UBXD1^{FLAG} and in both cases, UBXD1^{FLAG} staining overlapped with ERGIC-53. First, there was an increase in the percentage of ERGIC-53 protein present in cytoplasmic vacuoles (noted by arrows with dashed lines) (Fig. 6). This was observed in 50–60% of UBXD1^{FLAG} expressing cells. Second, we observed an enhancement in the amount of

ERGIC-53 localized close to or at the cell membrane in ~20% of UBXD1^{FLAG} positive cells (noted by arrows with solid lines). Cytoplasmic vacuole or membrane localization of ERGIC-53 was not observed in cells expressing UBXD1Δ10^{FLAG} (Fig. 6).

DISCUSSION

UBXD1 is a member of the non-UBA domain family of p97 adaptors and it has recently been shown to be defective at binding p97 mutants found in familial IBMPFD and ALS (10).

TABLE III
Spectral counts of proteins associated with ^{FLAG}ERGIC-53 in transiently transfected 293T cells as assessed by SILAC[a]

Proteins[b]	# of assigned spectra[c]
ER-Golgi intermediate compartment 53kDa protein (ERGIC-53)	495/209
Rab3 GTPase-activating noncatalytic subunit (RAB3GAP2)	84/23
Rab3 GTPase-activating catalytic subunit (RAB3GAP1)	71/51
Heat shock cognate 71 kDa protein (HSPA8)	60/100
Heat shock 70 kDa protein 1A/1B (HSPA1A,HSPA1B)	45/58
Coatomer subunit alpha (COPA)	43/22
cDNA FLJ54303, highly similar to Heat shock 70 kDa protein 1	43/58
Transitional endoplasmic reticulum ATPase (VCP)	35/27
Tubulin beta-2 chain (TUBB2C)	78/47
Tubulin beta-3 chain (TUBB3)	50/34
Coatomer subunit beta' (COPB2)	32/22
Tubulin beta-4 chain (TUBB4)	66/37
Tubulin beta-2A chain (TUBB2)	64/39
Tubulin beta chain (TUBB)	75/56
Coatomer subunit epsilon (COPE)	26/19
Coatomer subunit beta (COPB1)	23/17
DnaJ homolog subfamily C member 7 (DNAJC7)	19/14
Protein disulfide-isomerase (P4HB)	15/14

[a] Mass spectrometry was performed with LTQ-Orbitrap instrument.
[b] Peptides and proteins were filtered at a 1% false discovery rate.
[c] Inclusion limit set at a minimal of 10 spectra counts and all proteins were significantly enriched in replicate ($p < 0.05$ Bonferroni corrected).

These results indicate that processes requiring the activity of a p97-UBXD1 complex are altered in human disease and underscore the importance of elucidating its biochemical and molecular activities. To begin to uncover these functions, we used liquid chromatography mass spectrometry based approaches to identify interacting partners for UBXD1. We have found that UBXD1 interacts strongly with ERGIC-53, a molecule that functions in protein trafficking (reviewed in 26, 27). This interaction is very specific (not observed with other UBX proteins) and requires the amino-terminal domain of UBXD1 and the carboxy-terminal tail of ERGIC-53. Interestingly, UBXD1-ERGIC-53 interaction is suppressed by the p97 inhibitor DBeQ that blocks the ATPase activity of the enzyme (28). These results indicate that formation of a stable UBXD1-ERGIC-53 complex requires the enzymatic activity of p97. We have also found that UBXD1-ERGIC-53 association is unaffected by the E1 ubiquitin activation enzyme inhibitor. This suggests that UBXD1-ERGIC-53 interaction is not mediated by ubiquitination and indicates that the non-UBA family of p97 adaptors can couple p97 to substrates in an ubiquitin-independent manner.

What might be the biochemical consequence of these associations? Based on the data presented here, we propose that p97 and UBXD1 cooperate in regulating the association of trafficking factors with the C-terminal tails of hexameric ERGIC-53. P97 and UBXD1 may work together in displacing proteins that interact with the ERGIC-53 tails and/or promote the formation of new stable interactions, including with UBXD1 itself. As we find that Rab3GAP1 interacts with UBXD1 through ERGIC-53, it is possible that the tails of a single ERGIC-53 hexamer can link together different complexes that in cooperation modulate ERGIC-53 trafficking.

ERGIC-53 is known to cycle between the ER, ERGIC, and Golgi (reviewed in 26, 27). It has also been shown that upon transient overproduction, ERGIC-53 localizes to the cell surface, where it can subsequently undergo endocytosis (32). This cell surface localization was deemed aberrant and attributed to the saturation of cofactors required for intracellular retention (32). We would like to suggest that a pool of endogenous ERGIC-53 naturally localizes to the plasma membrane, perhaps in a regulated manner, and is recycled by endocyto-

TABLE IV
*Quantitative analysis of proteins associating with ^{FLAG}ERGIC-53 versus ^{FLAG}ERGIC-53ΔC[a]. *Indicates significant decrease in ^{FLAG}ERGIC-53ΔC immunoprecipitations ($p < 0.05$ Bonferroni corrected)*

Proteins[b]	# of assigned spectra	
	Heavy (^{FLAG}WT)	Light (^{FLAG}ΔC)
ER-Golgi intermediate compartment 53kDa protein (ERGIC-53)	*1019	671
Coatomer subunit alpha (COPA)*	17	0
Rab3 GTPase-activating catalytic subunit (RAB3GAP1)*	16	0
Coatomer subunit beta' (COPB2)	29	9
Rab3 GTPase-activating non-catalytic subunit (RAB3GAP2)	7	0
Coatomer subunit delta (COPD)	5	0
Coatomer subunit zeta-1 (COPZ1)	7	1

[a] Mass spectrometry was performed with LTQ-Orbitrap instrument.
[b] Peptides and proteins were filtered at a 1% false discovery rate.

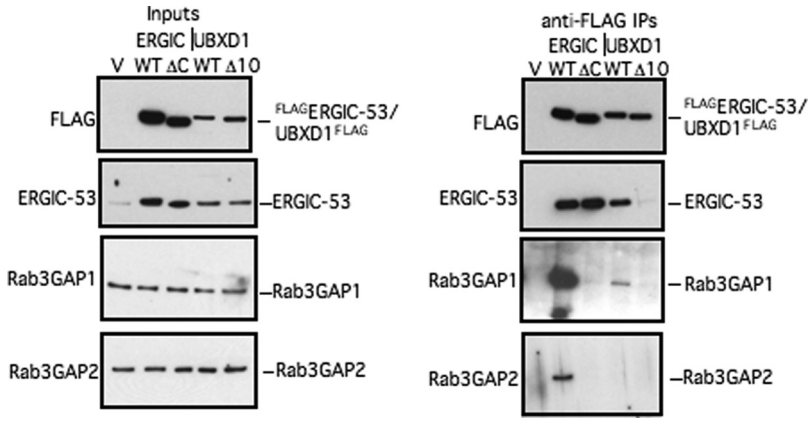

FIG. 5. **Defining domains of ERGIC-53 and UBXD1 required for interactions with Rab3GAP proteins by Western blotting and immunoprecipitation.** 293T cells were transfected with 2 μg of the indicated ^{FLAG}ERGIC-53 or UBXD1^{FLAG} expression constructs. Extracts were prepared and immunoprecipitations carried out with anti-FLAG beads. Western blots were performed with anti-FLAG, anti-ERGIC-53, Rab3GAP1, and Rab3GAP2 antibodies.

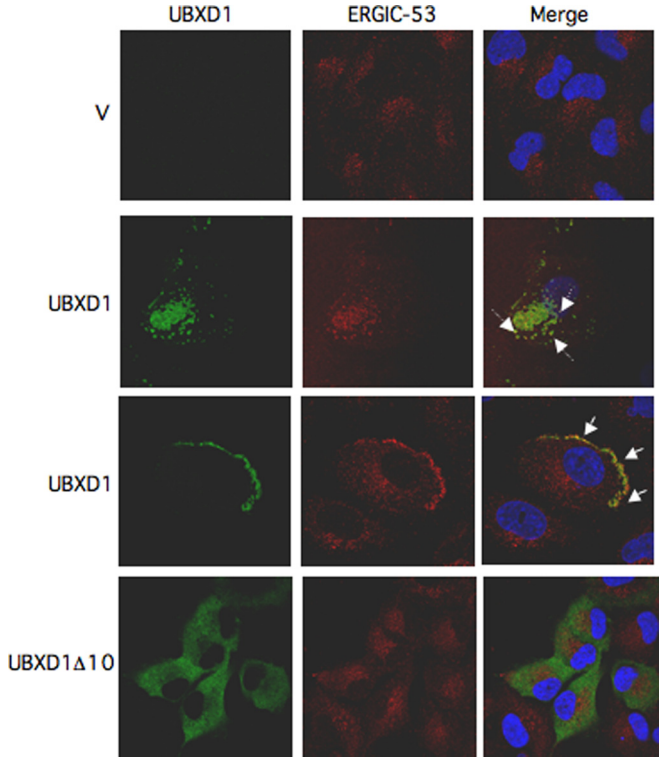

FIG. 6. **Effects of UBXD1 expression on localization of endogenous ERGIC-53.** H1299 cells harboring pIND (V) and pIND-UBXD1^{FLAG} were exposed to 1 μM of ponasterone for 48 h. ERGIC-53 and UBXD1^{FLAG} localization was assessed by indirect immunofluorescence and confocal microscopy using rabbit anti-ERGIC-53 polyclonal antibodies and the mouse anti-UBXD1 antibody 5C3-1.

sis. Three observations support this idea. First, proteomics studies have identified endogenous ERGIC-53 in purified early endosomes (33). Second, UBXD1 can promote the localization of endogenous ERGIC-53 to the cell periphery. Third, both transfected and endogenous ERGIC-53 (this is deduced based on detecting an interaction between UBXD1 and Rab3GAP1 that is dependent on the ERGIC-53 binding domain of the protein) bind Rab3GAPs, a protein complex involved in promoting vesicle fusion at the cell membrane (31). If this speculation is correct, it will be interesting to define protein constituents of vesicles that contain ERGIC-53 and Rab3GAPs and what functions they confer. A number of ERGIC-53 clients have been identified, including alpha-1 antitrypsin (34), coagulation factors V/VII (35), and cathepsin C (36) and Z (37). However, considering that these are luminal and/or secreted proteins as well as their trafficking are routed through the Golgi, it seems unlikely that a p97-UBXD1 complex is promoting the movement of these ERGIC-53 clients to the cell surface. Rather, p97-UBXD1 may induce cell surface trafficking of other integral or peripheral membrane proteins that are present on ERGIC-53 positive vesicles and perhaps function at the cell surface or on endocytosed vesicles. This could even pertain to p97 and UBXD1 themselves. Interestingly, p97 and UBXD1 have recently been reported to promote endo-lysosomal sorting of ubiquitinated caveolins (10). Perhaps ERGIC-53 plays a role in the routing of p97-UBXD1 so it can function in this process. Alternatively, p97-UBXD1 may not directly regulate ERGIC-53 localization, but influence how ERGIC-53 loaded with luminal ligands is packaged into transport vesicles that move to specific locations. This could be through controlling the association/disassociation with various transport factors with the C-terminal tails or regulating the oligomerization of ERGIC-53 by binding the tails. Future studies are obviously needed to work out the mechanistic consequences of these newly discovered interactions.

UBXD1 is defective at binding p97 mutants found in familial IBMPFD and ALS (10). It will therefore be important to test if trafficking of ERGIC-53 or ERGIC-53 containing vesicles are compromised in cells harboring mutant p97. ERGIC-53 is mutated in a rare autosomal recessive clotting disorder in which the amount of its client proteins coagulation factors V and VIII are diminished in the plasma (38). Most mutations reported to date lead to absence of ERGIC-53 protein and there has yet to be any report of other abnormalities in these individuals. It is therefore unlikely that loss of ERGIC-53 function alone is causal for IBMPFD and ALS phenotypes in patients with mutant p97. A recent study has shown that deletion of ERGIC-53 alleles in mice results in a modest decrease in factor V and VII levels in the serum and interestingly, a partially penetrant, perinatal embryonic lethality (39). Thus,

ERGIC-53 is likely to have yet to be discovered functions that are influenced by polymorphic alleles. If so, the presence of these alleles in situations of defective p97-UBXD1 regulated ERGIC-53 trafficking may contribute to IBMPFD and/or ALS. Alternatively, loss of p97-UBXD1 function may result in a gain of ERGIC-53 activity that promotes these diseases. Future experiments using loss of functional approaches will address the functional role of p97-UBXD1 in the trafficking of ERGIC-53 and ERGIC-53 containing vesicles and if these processes are disturbed in cells harboring mutant p97. As UBXD1 shows high expression in neurons (40), it is likely that these cells will be the most appropriate for future studies investigating the role of UBXD1 in modulating the trafficking of ERGIC-53 containing vesicles, defining how this activity impinges on cellular processes, and determining if alterations in this pathway contribute to neurodegeneration.

Acknowledgments—DSH thanks his Department and Institute Chairs for permission to perform summer work at Caltech.

* DSH acknowledges support from the Fels Institute for Cancer Research and Molecular Biology and the Temple University Faculty Senate Seed funds. JEL was supported by the Ruth L. Kirschstein NRSA fellowship CA138126 whereas WBD was supported by the Ruth L. Kirschstein NRSA fellowship GM088975. The Proteome Exploration Lab was supported by the Beckman Institute at Caltech and an award from the Gordon and Betty Moore Foundation. RJD is an Investigator of the Howard Hughes Medical Institute and this work was supported in part by HHMI.

S This article contains supplemental Tables S1 to S5.

** To whom correspondence should be addressed: Fels Institute for Cancer Research and Molecular Biology Temple, University School of Medicine, 3307 North Broad Street, Philadelphia PA 19104. E-mail: dhaines@temple.edu.

REFERENCES

1. Watts, G. D., Wymer, J., Kovach, M. J., Mehta, S. G., Mumm, S., Darvish, D., Pestronk, A., Whyte, M. P., and Kimonis, V. E. (2004) Inclusion body myopathy associated with Paget disease of bone and frontotemporal dementia is caused by mutant valosin-containing protein. *Nat. Genet.* **36,** 377–381
2. Johnson, J. O., Mandrioli, J., Benatar, M., Abramzon, Y., Van Deerlin, V. M., Trojanowski, J. Q., Gibbs, J. R., Brunetti, M., Gronka, S., Wuu, J., Ding, J., McCluskey, L., Martinez-Lage, M., Falcone, D., Hernandez, D. G., Arepalli, S., Chong, S., Schymick, J. C., Rothstein, J., Landi, F., Wang, Y. D., Calvo, A., Mora, G., Sabatelli, M., Monsurrò, M. R., Battistini, S., Salvi, F., Spataro, R., Sola, P., Borghero, G.; ITALSGEN Consortium, Galassi, G., Scholz, S. W., Taylor, J. P., Restagno, G., Chiò, A., and Traynor, B. J. (2010) Exome sequencing reveals VCP mutations as a cause of familial ALS. *Neuron* **68,** 857–864
3. Uchiyama, K., and Kondo, H. (2005) p97/p47-Mediated biogenesis of Golgi and ER. *J. Biochem.* **137,** 115–119
4. Wolf, D. H., and Stolz, A. (2011) The Cdc48 machine in endoplasmic reticulum associated protein degradation. *Biochim. Biophys. Acta* Jul 23. [Epub ahead of print].
5. Dargemont, C., and Ossareh-Nazari, B. (2011) Cdc48/p97, a key actor in the interplay between autophagy and ubiquitin/proteasome catabolic pathways. *Biochim. Biophys. Acta* Jul 23. [Epub ahead of print].
6. Yamanaka, K., Sasagawa, Y., and Ogura, T. (2011) Recent advances in p97/VCP/Cdc48 cellular functions. *Biochim. Biophys. Acta* Jul 12. [Epub ahead of print].
7. Meyer, H., and Popp, O. (2008) Role(s) of Cdc48/p97 in mitosis. *Biochem. Soc. Trans.* **36,** 126–130
8. Ju, J. S., Fuentealba, R. A., Miller, S. E., Jackson, E., Piwnica-Worms, D., Baloh, R. H., and Weihl, C. C. (2009) Valosin-containing protein (VCP) is required for autophagy and is disrupted in VCP disease. *J. Cell Biol.* **187,** 875–888
9. Tresse, E., Salomons, F. A., Vesa, J., Bott, L. C., Kimonis, V., Yao, T. P., Dantuma, N. P., and Taylor, J. P. (2010) VCP/p97 is essential for maturation of ubiquitin-containing autophagosomes and this function is impaired by mutations that cause IBMPFD. *Autophagy* **6,** 217–227
10. Ritz, D., Vuk, M., Kirchner, P., Bug, M., Schütz, S., Hayer, A., Bremer, S., Lusk, C., Baloh, R. H., Lee, H., Glatter, T., Gstaiger, M., Aebersold, R., Weihl, C. C., and Meyer, H. (2011) Endolysosomal sorting of ubiquitylated caveolin-1 is regulated by VCP and UBXD1 and impaired by VCP disease mutations. *Nat. Cell Biol.* **13,** 1116–1123
11. Ernst, R., Mueller, B., Ploegh, H. L., and Schlieker, C. (2009) The otubain YOD1 is a deubiquitinating enzyme that associates with p97 to facilitate protein dislocation from the ER. *Mol. Cell* **36,** 28–38
12. Koegl, M., Hoppe, T., Schlenker, S., Ulrich, H. D., Mayer, T. U., and Jentsch, S. (1999) A novel ubiquitination factor, E4, is involved in multiubiquitination chain assembly. *Cell* **96,** 635–644
13. Rabinovich, E., Kerem, A., Fröhlich, K. U., Diamant, N., and Bar-Nun, S. (2002) AAA-ATPase p97/Cdc48p, a cytosolic chaperone required for endoplasmic reticulum-associated protein degradation. *Mol. Cell. Biol.* **22,** 626–634
14. Shcherbik, N., and Haines, D. S. (2007) Cdc48p(Np14p/Ufd1p) binds and segregates membrane-anchored/tethered complexes via a polyubiquitin signal present on the anchors. *Mol. Cell* **25,** 385–397
15. Meyer, H. H., Wang, Y., and Warren, G. (2002) Direct binding of ubiquitin conjugates by the mammalian p97 adaptor complexes, p47 and Ufd1-Npl4. *EMBO J.* **21,** 5645–5652
16. Madsen, L., Seeger, M., Semple, C. A., and Hartmann-Petersen, R. (2009) New ATPase regulators–p97 goes to the PUB. *Int. J. Biochem. Cell Biol.* **41,** 2380–2388
17. Yeung, H. O., Kloppsteck, P., Niwa, H., Isaacson, R. L., Matthews, S., Zhang, X., and Freemont, P. S. (2008) Insights into adaptor binding to the AAA protein p97. *Biochem. Soc. Trans.* **36,** 62–67
18. Schuberth, C., and Buchberger, A. (2008) UBX domain proteins: major regulators of the AAA ATPase Cdc48/p97. *Cell Mol. Life Sci.* **65,** 2360–2371
19. Alexandru, G., Graumann, J., Smith, G. T., Kolawa, N. J., Fang, R., and Deshaies, R. J. (2008) UBXD7 binds multiple ubiquitin ligases and implicates p97 in the H1F1alpha turnover. *Cell* **134,** 804–816
20. Halawani, D., LeBlanc, A. C., Rouiller, I., Michnick, S. W., Servant, M. J., and Latterich, M. (2009) Hereditary inclusion body myopathy-linked p97/VCP mutations in the NH2 domain and the D1 ring modulate p97/VCP ATPase activity and D2 ring conformation. *Mol. Cell. Biol.* **29,** 4484–4494
21. Fernández-Sáiz, V., and Buchberger, A. (2010) Imbalances in p97 co-factor interactions in human proteinopathy. *EMBO Rep.* **11,** 479–485
22. Ramkumar, P., Smith, B. A., Akinbamidele, A. C., Kapcia, J., Beauparlant, S. L., and Haines, D. S. (2009) Generation and characterization of novel monoclonal antibodies recognizing UBXD1. *Hybridoma* **28,** 459–462
23. Lee, J. E., Sweredoski, M. J., Graham, R., Ll Kolawa, N. J., Smith, G. T., Hess, S., and Deshaies, R. J. (2011) The steady-state repertoire of human SCF ubiquitin ligase complexes does not require ongoing Nedd8 conjugation. *Mol. Cell. Proteomics* **10,** M110.006460
24. Cox, J., and Mann, M. (2008) MaxQuant enables high peptide identification rates, individualized p.p.b.-range mass accuracies and proteome-wide quantification. *Nat. Biotechnol.* **26,** 1367–1372
25. Cox, J., Neuhauser, N., Michalski, A., Scheltema, R. A., Olsen, J. V., and Mann, M. (2011) Andromeda: A Peptide Search Engine Integrated into the MaxQuant Environment. *J. Proteome Res.* **10,** 1794–1805
26. Zhang, Y. C., Zhou, Y., Yang, C. Z., and Xiong, D. S. (2009) A review of ERGIC-53: its structure, functions, regulation and relations with diseases. *Histol. Histopathol.* **24,** 1193–1204
27. Hauri, H. P., Kappeler, F., Anderson, H., and Appenzeller, C. (2000) ERGIC-53 and traffic in the secretory pathway. *J. Cell Science* **113,** 587–596
28. Chou, T. F., Brown, S. J., Minond, D., Nordin, B. E., Li, K., Jones, A. C., Chase, P., Porubsky, P. R., Stoltz, B. M., Schoenen, F. J., Patricelli, M. P., Hodder, P., Rosen, H., and Deshaies, R. J. (2011) Reversible inhibitor of p97, *DBeQ,* impairs both ubiquitin-dependent and autophagic protein clearance pathways. *Proc. Natl. Acad. Sci. U.S.A.* **108,** 4834–4839

29. Yang, Y., Kitagaki, J., Dai, R. M., Tsai, Y. C., Lorick, K. L., Ludwig, R. L., Pierre, S. A., Jensen, J. P., Davydov, I. V., Oberoi, P., Li, C. C., Kenten, J. H., Beutler, J. A., Vousden, K. H., and Weissman, A. M. (2007) Inhibitors of ubiquitin-activating enzyme (E1), a new class of potential cancer therapeutics. *Cancer Res.* **67,** 9472–9481
30. Scales, S. J., Pepperkok, R., and Kreis, T. E. (1997) Visualization of ER-to-Golgi transport in living cells reveals a sequential mode of action for COPII and COPI. *Cell* **90,** 1137–1148
31. Müller, M., Pym, E. C., Tong, A., and Davis, G. W. (2011) Rab3-GAP controls the progression of synaptic homeostasis at a late stage of vesicle release. *Neuron* **69,** 749–762
32. Kappeler, F., Itin, C., Schindler, R., and Hauri, H. P. (1994) A dual role for COOH-terminal lysine residues in pre-Golgi retention and endocytosis of ERGIC-53. *J. Biol. Chem.* **269,** 6279–6281
33. Foster, L. J., de Hoog, C. L., Zhang, Y., Zhang, Y., Xie, X., Mootha, V. K., and Mann, M. (2006) A mammalian organelle map by protein correlation profiling. *Cell* **125,** 187–199
34. Nyfeler, B., Reiterer, V., Wendeler, M. W., Stefan, E., Zhang, B., Michnick, S. W., and Hauri, H. P. (2008) Identification of ERGIC-53 as an intracellular transport receptor of alpha1-antitrypsin. *J. Cell Biol.* **180,** 705–712
35. Nishio, M., Kamiya, Y., Mizushima, T., Wakatsuki, S., Sasakawa, H., Yamamoto, K., Uchiyama, S., Noda, M., McKay, A. R., Fukui, K., Hauri, H. P., and Kato, K. (2010) Structural basis for the cooperative interplay between the two causative gene products of combined V and factor VII deficiency. *Proc. Natl. Acad. Sci. U.S.A.* **107,** 4034–4039
36. Vollenweider, F., Kappeler, F., Itin, C., and Hauri, H. P. (1998) Mistargeting of the lectin ERGIC-53 to the endoplasmic reticulum of HeLa cells impairs the secretion of a lysosomal enzyme. *J. Cell Bio.* **142,** 377–389
37. Appenzeller, C., Andersson, H., Kappeler, F., and Hauri, H. P. (1999) The lectin ERGIC-53 is a cargo receptor for glycoproteins. *Nat. Cell Biol.* **1,** 330–334
38. Spreafico, M., and Peyvandi, F. (2009) Combined Factor V and Factor VIII Deficiency. *Semin. Thromb. Hemost.* **35,** 390–399
39. Zhang, B., Zheng, C., Zhu, M., Tao, J., Vasievich, M. P., Baines, A., Kim, J., Schekman, R., Kaufman, R. J., and Ginsburg, D. (2011) Mice deficient in LMAN1 exhibit FV and FVIII deficiencies and liver accumulation of α1-antitrypsin. *Blood* **118,** 3384–3391
40. Madsen, L., Andersen, K. M., Prag, S., Moos, T., Semple, C. A., Seeger, M., and Hartmann-Petersen, R. (2008) Ubxd1 is a novel co-factor of the human p97 ATPase. Int J Biochem. *Int. J. Biochem. Cell Biol.* **40,** 2927–2942